Commun. Theor. Phys. (Beijing, China) **47** (2007) pp. 349–354

Vol. 47, No. 2, February 15, 2007

Vibration Spectra of Quasi-confined Optical Phonon Modes in an Asymmetric Wurtzite $Al_xGa_{1-x}N/GaN/Al_yGa_{1-y}N$ Quantum Well*

ZHANG Li[1,2] and SHI Jun-Jie[1]

[1]State Key Laboratory for Mesoscopic Physics and School of Physics, Peking University, Beijing 100871, China

[2]Department of Mechanics and Electronics, Panyu Polytechnic, Panyu 511483, China†

(Received March 6, 2006; Revised April 26, 2006)

Abstract *Based on the dielectric continuum model and Loudon's uniaxial crystal model, the properties of the quasi-confined (QC) optical phonon dispersions and the electron-QC phonons coupling functions in an asymmetric wurtzite quantum well (QW) are deduced via the method of electrostatic potential expanding. The present theoretical scheme can naturally reduce to the results in symmetric wurtzite QW once a set of symmetric structural parameters are chosen. Numerical calculations on an asymmetric AlN/GaN/$Al_{0.15}Ga_{0.85}N$ wurtzite QW are performed. A detailed comparison with the symmetric wurtzite QW was also performed. The results show that the structural asymmetry of wurtzite QW changes greatly the dispersion frequencies and the electrostatic potential distributions of the QC optical phonon modes.*

PACS numbers: 78.67.De, 63.20.Dj, 74.25.Kc
Key words: quasi-confined optical phonon, asymmetric wurtzite QW, nitride-based semiconductor

1 Introduction

In recent years, a considerable amount of research has been devoted to electronic and optical properties of quantum well (QW) based on wurtzite GaN, AlN, InN, and their ternary compounds $Al_xGa_{1-x}N$ and $In_xGa_{1-x}N$.[1−6] This is mainly due to their wide direct band-gaps covering from ultraviolet to red, which results in their potential device application for high-brightness blue/green light emitting diodes and laser diodes. The group-III nitrides usually crystallize in wurtzite structure, which makes their phonon spectra become much more complex due to anisotropy of the crystal structure compared with phonons in cubic crystals.[2−7] Hence it is very important and necessary to understand the lattice dynamics and electron-phonon interactions in wurtzite quantum heterostructures.

Since the pioneer work of Licari[8] and Fuchs[9] on the polar phonon modes in confined quantum systems, several theoretical models, such as the dielectric continuum (DC) models, the microscopic calculation models, the hydrodynamic models, and Huang–Zhu models have been proposed successively.[10−15] The microscopic calculation model[10,11] is the principal model based on first-principles interatomic force constants. The DC model[12] uses the electrostatic boundary conditions (BCs), while the hydrodynamic model[13,14] adopts mechanical BCs at the interfaces. But both of the two models have demerit for the description of the optical phonons in quantum confined systems, namely, the discontinuous mechanical BCs for DC model and discontinuous electric BCs for hydrodynamic model. The Huang–Zhu model[15] takes into account both of the electrostatic and mechanical BCs, i.e., the continuity of the tangential component of the electric field, the normal component of electric displacement vector, and the relative ionic displacement field at the heterointerfaces. However, as pointed out by Klimin *et al.*,[16] the choice of the BC becomes less critical if the observed physical quantities include sum over all phonon modes. Moreover, the calculation results of the phonon spectra and electron-phonon scattering based on the DC model agree well with those of microscopic model.[17] Hence the DC model is widely employed in recent literature due to its validity and simplicity. On the basis of the DC model and the Loudon's uniaxial crystal model, the works of polar phonon modes have been successfully extended from the cubic-crystal QWs to the wurtzite nitride QW systems.[2−6] For example, Shi[5] solved exactly the equation of motion for the p-polarization field in an arbitrary wurtzite multilayer heterostructure by using transfer matrix method, whose results reveal that five types of optical phonons including the interface optical (IO) modes, the propagating modes, quasi-confined (QC) modes, the exactly confined modes, and the half-space (HS) modes, coexist in the wurtzite multilayer quantum systems. After that work,[5] Li *et al.*[6] further studied the dispersion properties of the QC optical phonon modes in multilayer wurtzite QWs, but only the symmetric wurtzite AlN/GaN/AlN QWs were numerically analyzed.

The vibration properties of lattice vibration as well as relative optical characteristic in wurtzite GaN-based QWs and super-lattices (SLs) have been extensively investigated in experiments.[18−21] For example, Sun *et al.*[18] have demonstrated the large coherent longitudinal-acoustic (LA) phonon oscillations[19] in InGaN/GaN multiple QWs via UV femtosecond pulse excitation. Martinez and coworkers[20] have also observed the terahertz coherent LA phonons in a GaN/AlN SL by employing femtosecond laser excitation and bolometric detection techniques. Through the impulsive Raman scattering, the coherent phonon modes of A_1(LO), high- and low-frequency E_2 were revealed in bulk GaN materials in Yee's

*The project supported by National Natural Science Foundation of China under Grant Nos. 60276004 and 60390073, the Scientific Research Foundation for the Returned Ooverseas Chinese Scholars, State Education Ministry of China

†Mailing address

experiment.[21] These results have great importance for explanation and analysis of the optical properties and other physical characteristic with polar phonons participation in wurtzite nitride-based heterostructures.

All of the aforementioned theoretical works[2−6] dealt with the optical phonon modes in symmetric wurtzite quantum systems. However, to the best of our knowledge, there is rare work considering the lattice dynamic properties in asymmetric wurtzite heterostructure systems. In fact, Im *et al.*[22] have measured the confined effects of carrier in an asymmetric wurtzite GaInN/AlGaN/GaN QWs, and their result reveals that oscillator strength has been enhanced in the asymmetric structure, which indicates better carrier confinement in such asymmetric structure relative to the symmetric one. Furthermore, Shi[23] and Kinsler[24] theoretically analyzed the confined and IO phonon modes as well as their influences on the electron-phonon scattering in asymmetric cubic GaAs/Al_xGa_{1-x}As QWs, respectively. Their results show obviously different vibrational properties of phonon modes and corresponding characteristic of electron-phonon coupling. Stavrou and coauthors[25] calculated and compared the electron capture rates in symmetric and asymmetric CdSe QWs, and they also obtained the important conclusion that the capture rate in asymmetric structure exhibites some interesting features other than in symmetric structure. Moreover, the asymmetric quantum systems have great applications in nonlinear optoelectronic devices based on the optical rectification, electro-optics effect, and second-harmonic generations.[26−28] Therefore, it is necessary to investigate the lattice dynamic properties in the asymmetric wurtzite systems.

Motivated by the work of QC phonon modes in symmetric wurtzite QWs,[6] we present a theoretical analysis of the properties of the QC phonon modes in a wurtzite asymmetric QW in the current paper. The main significance of this work is as follows. (i) Via the method of the electrostatic potential expanding, the free QC phonon field and corresponding Fröhlich electron-phonon interaction Hamiltonian in an asymmetric wurtzite QW have been derived. In fact, our theory can be looked on as the general one for the QC optical phonons in wurtzite QW, and it can reduce to the symmetric case once a set of symmetric parameters are chosen.[6] (ii) The QC phonon dispersion and the electron QC phonon coupling functions have been calculated and analyzed, and a detailed comparison with those in symmetric wurtzite QW systems has been exhibited. (iii) The present theoretical scheme and numerical results are important and useful for further experimental and theoretical investigations of the QC phonon effects on some complicated asymmetric wurtzite QW structures, such as the influence of QC phonons on the second-order nonlinearity in the asymmetric wurtzite QW systems.[26−28]

2 Theory

Considering an asymmetric wurtzite $Al_xGa_{1-x}N$ /GaN/$Al_yGa_{1-y}N$ ($x \neq y$) QW model with the two heterostructures located at $z = \pm d$, we take the z-axis along the direction of the c-axis of the wurtzite material and denote the radial directions as t. Due to the anisotropy of wurtzite crystals, the polar phonon frequencies and the dielectric function become direction-dependent and the latter is given by[2−6]

$$\epsilon_i(\omega) = \begin{pmatrix} \epsilon_{ti}(\omega) & 0 & 0 \\ 0 & \epsilon_{ti}(\omega) & 0 \\ 0 & 0 & \epsilon_{zi}(\omega) \end{pmatrix}, \tag{1}$$

where

$$\epsilon_{ti}(\omega) = \epsilon_{ti}^{\infty} \frac{\omega^2 - \omega_{t,Li}^2}{\omega^2 - \omega_{t,Ti}^2},$$

$$\epsilon_{zi}(\omega) = \epsilon_{zi}^{\infty} \frac{\omega^2 - \omega_{z,Li}^2}{\omega^2 - \omega_{z,Ti}^2}, \quad i = 1, 2, 3. \tag{2}$$

Here $\omega_{z,L}$, $\omega_{z,T}$, $\omega_{t,L}$, and $\omega_{t,T}$ are the zone center characteristic frequencies of A_1(LO), A_1(TO), E_1(LO), and E_1(TO) modes, respectively. The subscript $i = 1$, 2, and 3 denotes the $Al_xGa_{1-x}N$, GaN, and $Al_yGa_{1-y}N$ materials, respectively. Within the framework of Loudon's uniaxial crystal model, their dispersion relation for the extraordinary phonons in a wurtzite bulk material is described by[5]

$$\epsilon_t(\omega) k_t^2 + \epsilon_z(\omega) k_z^2 = 0. \tag{3}$$

Here k_z (k_t) is the phonon wave number in free z-direction (t-direction) and ω is the frequency of polar phonon. Without loss of generality, both k_t and ω can be chosen as real and positive numbers.[2−5] Based on the discussion in Refs. [2] ∼ [6], we know that, when $\epsilon_t(\omega)\epsilon_z(\omega) < 0$, the phonon modes correspond to the oscillating waves. On the contrary, they correspond to the decaying ones when $\epsilon_t(\omega)\epsilon_z(\omega) > 0$. In the next discussion, we will only focus our attention on the QC optical phonon modes for simplicity in the present paper. For convenience, we define a function γ_i as

$$\gamma_i(\omega) = \mathrm{sign}\Big[\frac{\epsilon_{ti}(\omega)}{\epsilon_{zi}(\omega)}\Big] \sqrt{\Big|\frac{\epsilon_{ti}(\omega)}{\epsilon_{zi}(\omega)}\Big|}, \quad i = 1, 2, 3. \tag{4}$$

Let us discuss the frequency range where the QC phonon modes exist. In Fig. 1, the function $\gamma_i(\omega)$ as a function of ω is plotted. The subscript $i = 1$, 2, and 3 corresponds to the AlN, GaN, and $Al_{0.15}Ga_{0.85}N$ materials, respectively. For the QC phonon modes, the function $\gamma_i(\omega)$ ($i = 1$, 3) should have positive values, and $\gamma_2(\omega)$ should be negative value. The electrostatic potential of the QC phonons could thus be oscillating waves in the well-layer material and be decaying waves in the barrier-layer materials, which is similar to that of electrons confined in a QW of finite depth.[5,6] It is obviously observed from the figure that, the frequencies of QC phonon modes in the wurtzite AlN/GaN/$Al_{0.15}Ga_{0.85}N$

QW must fall into the two ranges, i.e., $\omega_{z,T2}$-$\omega_{z,T3}$ and $\omega_{z,L2}$-$\omega_{t,L2}$.

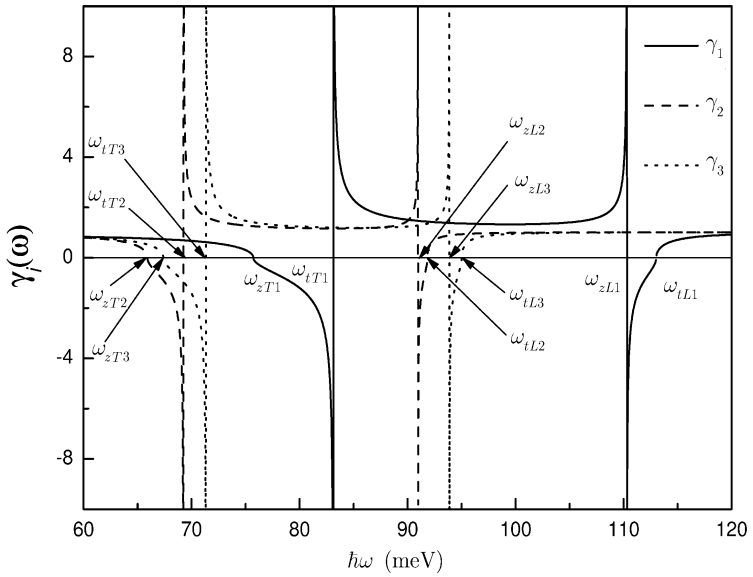

Fig. 1 The function $\gamma_i(\omega)$ as a function of ω. $\gamma_i(\omega)$ $(i = 1, 2, 3)$ correspond to the AlN, GaN, and $Al_{0.15}Ga_{0.85}N$ materials, respectively.

Considering the case of free oscillations (the charge density $\rho_0(\boldsymbol{r}) = 0$) in the media and using the Maxwell equations, the electrostatic potential of QC phonon modes can thus be written as[2−4]

$$\begin{aligned}\Phi(\boldsymbol{r}) = \Phi(\rho, z) &= \mathrm{e}^{\mathrm{i}k_t\cdot\rho}\phi(z)\\ &= \sum_{k_t}\mathrm{e}^{\mathrm{i}k_t\cdot\rho}\times\begin{cases} A_1\exp(\gamma_1 k_t z), & -\infty < z \leqslant -d\,,\\ A_2\cos(\gamma_2 k_t z) + B_2\sin(\gamma_2 k_t z), & -d < z \leqslant d\,,\\ B_3\exp(-\gamma_3 k_t z), & d < z < \infty\,.\end{cases}\end{aligned} \tag{5}$$

Using the boundary continuity conditions of the phonon potential functions and their normal components of electric displace at the interfaces $z = \pm d$, the dispersion relation equation of the QC phonon modes in the three-layer asymmetric wurtzite QWs has been obtained, and it is given by

$$\tan[2\gamma_2 k_t d\,] = \frac{\gamma_2\epsilon_{z,2}(\gamma_1\epsilon_{z,1} + \gamma_3\epsilon_{z,3})}{\gamma_2^2\epsilon_{z,2}^2 - \gamma_1\gamma_3\epsilon_{z,1}\epsilon_{z,3}}\,. \tag{6}$$

In particular, for the symmetric wurtzite QW, i.e. $\gamma_1 = \gamma_3$ and $\epsilon_{z,1} = \epsilon_{z,3}$, then equation (6) can be further simplified, and it is given as

$$\tan[2\gamma_2 k_t d\,] = 2\Big(\frac{\gamma_2\epsilon_{z,2}}{\gamma_1\epsilon_{z,1}} - \frac{\gamma_1\epsilon_{z,1}}{\gamma_2\epsilon_{z,2}}\Big)^{-1} = 2\left(\sqrt{\left|\frac{\epsilon_{t,2}\epsilon_{z,2}}{\epsilon_{t,1}\epsilon_{z,1}}\right|} - \sqrt{\left|\frac{\epsilon_{t,1}\epsilon_{z,1}}{\epsilon_{t,2}\epsilon_{z,2}}\right|}\right)^{-1}\,. \tag{7}$$

Equation (7) is just the dispersion relation equation of QC phonon modes in a symmetric wurtzite AlN/GaN/AlN QW.[6] This means that the present theories for the description of the QC optical phonons in asymmetric wurtzite QW are more general than the symmetrical ones.

Using a similar quantization step to the IO phonons in wurtzite and cubic quantum systems,[5−7] we get the free QC phonon field Hamiltonian as

$$H_{\mathrm{QC}} = \sum_{\boldsymbol{k}_t}\hbar\omega\Big(b^{\dagger}_{\boldsymbol{k}_t}b_{\boldsymbol{k}_t} + \frac{1}{2}\Big)\,, \tag{8}$$

where $b^{\dagger}_{\boldsymbol{k}_t}$ and $b_{\boldsymbol{k}_t}$ are creation and annihilation boson operators for QC phonon of the $\boldsymbol{k}_t$-th mode. The Fröhlich Hamiltonian describing the interaction between an electron and the QC optical phonons is given by

$$H_{e-\mathrm{QC}} = -\sum_{\boldsymbol{k}_t}\Gamma^{\mathrm{QC}}_{\boldsymbol{k}_t}(z)[b_{\boldsymbol{k}_t}\,\mathrm{e}^{\mathrm{i}\boldsymbol{k}_t\cdot\boldsymbol{\rho}} + \mathrm{H.c.}]\,, \tag{9}$$

where $\Gamma^{\mathrm{QC}}_{\boldsymbol{k}_t}(z)$ is the coupling function defined as

$$\Gamma^{\mathrm{QC}}_{\boldsymbol{k}_t}(z) = N_{\boldsymbol{k}_t}\times\begin{cases} g_1\exp(\gamma_1 k_t z), & -\infty < z \leqslant -d\,,\\ g_2\cos(\gamma_2 k_t z) + g_3\sin(\gamma_2 k_t z), & -d < z \leqslant d\,,\\ g_4\exp(-\gamma_3 k_t z), & d < z < \infty\,,\end{cases} \tag{10}$$

where

$$
\begin{aligned}
g_1 &= -\gamma_2\epsilon_{z,2}\exp[-k_t\gamma_3 d]\,,\\
g_2 &= \exp[-(\gamma_1+\gamma_3)k_t d][\gamma_1\epsilon_{z,1}\sin(k_t\gamma_2 d)+\gamma_2\epsilon_{z,2}\cos(k_t\gamma_2 d)]\,,\\
g_3 &= \exp[-(\gamma_1+\gamma_3)k_t d][\gamma_2\epsilon_{z,2}\sin(k_t\gamma_2 d)-\gamma_1\epsilon_{z,1}\cos(k_t\gamma_2 d)]\,,\\
g_4 &= -\exp(-\gamma_1 k_t d)[\gamma_1\epsilon_{z,1}\sin(2k_t\gamma_2 d)+\gamma_2\epsilon_{z,2}\cos(2k_t\gamma_2 d)]\,,
\end{aligned}
\tag{11}
$$

and

$$
\begin{aligned}
|N_{\boldsymbol{k}_t}| = \sqrt{\frac{4\pi\hbar\omega e^2}{k_t S}}\{&(\bar{\epsilon}_{t1}+\gamma_1^2\bar{\epsilon}_{z1})g_1^2\exp(-2\gamma_1 k_t d)/\gamma_1+2k_t(\bar{\epsilon}_{t2}+\gamma_2^2\bar{\epsilon}_{z2})(g_2^2+g_3^2)d\\
&+(\bar{\epsilon}_{t2}-\gamma_2^2\bar{\epsilon}_{z2})(g_2^2-g_3^2)\sin(2\gamma_2 k_t d)/\gamma_2+(\bar{\epsilon}_{t3}+\gamma_3^2\bar{\epsilon}_{z3})g_4^2\exp(-2\gamma_3 k_t d)/\gamma_3\}^{-1/2}\,.
\end{aligned}
\tag{12}
$$

In Eq. (12), $\bar{\epsilon}_{u,v}$ ($u=t,\ z$; $v=1,2,3$) is the effective dielectric constant, and it is defined by

$$
\bar{\epsilon}_{u,v} = \Big(\frac{1}{\epsilon_{u,v}-\epsilon_{u,v0}}-\frac{1}{\epsilon_{u,v}-\epsilon_{u,v\infty}}\Big)^{-1},\quad u=t,\ z;\ v=1,2,3\,. \tag{13}
$$

3 Numerical Results and Discussions

We have calculated the dispersion frequencies of the QC optical phonons and the electron-QC phonon coupling function for an asymmetric wurtzite AlN/GaN/$Al_{0.15}Ga_{0.85}N$ QW with the widths $\infty/4$ nm/∞. The material parameters used in our calculations are listed in Table 1.[2,5]

Table 1 Zone-center energies (in meV) of poloar phonons, and optical and static dielectric constant of wertzite AlN, GaN, and $Al_{0.15}Ga_{0.85}N$.[2,5]

Material	A_1(TO)	E_1(LO)	A_1(LO)	E_1(LO)	ϵ_∞	ϵ_0
AlN	75.72	83.13	110.30	113.02	4.77	8.5
GaN	65.91	69.25	90.97	91.93	5.35	9.2
$Al_{0.15}Ga_{0.85}N$	67.382	71.332	93.870	95.009	5.253	9.095

Figure 2 shows the dispersion frequencies $\hbar\omega$ of the QC phonon modes as a function of the phonon wave-number k_t in the asymmetric wurtzite QW system. From the figure, it can be seen that the QC optical phonon modes exist in the two regions: $\omega_{z,T2}$–$\omega_{z,T3}$ and $\omega_{z,L2}$–$\omega_{t,L2}$. This is completely consistent with the discussion of $\gamma_i(\omega)$ in Fig. 1. The higher frequency branches in $\omega_{z,L2}$–$\omega_{t,L2}$ are labelled by iH ($i=1,2,3,\ldots$), and the lower frequency branches in the frequency range $\omega_{z,T2}$–$\omega_{z,T3}$ are labelled by iL ($i=1,2,3,\ldots$). All the higher frequency branches are the monotonic and incremental functions of the phonon wave-number k_t, while all the low frequency ones are the monotonic and degressive functions of k_t. When k_t is small, the dispersion of each branch of QC phonon modes is more obvious. Furthermore, the figure also reveals the dispersion of the QC modes with small quantum number i is more dispersive than the modes with large i. Our calculation shows that, for a certain k_t, the dispersion equation (6) usually has infinite solutions for ω in the range $\omega_{z,L2}$–$\omega_{t,L2}$, which means that there are infinite branches of QC modes in the higher frequency range. This is quite similar to the case in the symmetric AlN/GaN/AlN wurtzite QW.[6] But the equation (6) usually has finite solutions for ω in the range $\omega_{z,T2}$–$\omega_{z,T3}$ for a definite k_t, which means that only finite branches of QC modes exist in the low frequency range in an asymmetric AlN/GaN/$Al_{0.15}Ga_{0.85}N$ QW. As k_t increases, the number of lower frequency QC branches will increase. This feature is obviously different from that in symmetric wurtzite QW,[6] which is completely due to their different symmetries. In fact, the low frequency range of QC modes in symmetric AlN/GaN/AlN QW is $\omega_{zT,\mathrm{GaN}}$–$\omega_{tT,\mathrm{GaN}}$, while that in asymmetric AlN/GaN/$Al_{0.15}Ga_{0.85}N$ QW is $\omega_{zT,\mathrm{GaN}}$–$\omega_{tT,\mathrm{Al_{0.15}Ga_{0.85}N}}$. Thus the dispersion curves of low frequency branches in asymmetric QW may be obtained via cutting off the dispersion frequency range of $\omega_{tT,\mathrm{Al_{0.15}Ga_{0.85}N}}$–$\omega_{tT,\mathrm{GaN}}$ in symmetric QW.[6] Via Fig. 1 or Eq. (4), it is clear to see that $\gamma_3(\omega)$ takes a negative value within the range $\omega_{tT,\mathrm{Al_{0.15}Ga_{0.85}N}}$–$\omega_{tT,\mathrm{GaN}}$, then the QC mode cannot exist in $\omega_{tT,\mathrm{Al_{0.15}Ga_{0.85}N}}$–$\omega_{tT,\mathrm{GaN}}$ in the asymmetric QW. The QC optical phonon modes will reduce to other oscillating modes, such as propagating optical phonon modes and HS modes.[5] This result clearly illustrates that the structural asymmetry has great influence on the dispersion of

QC optical phonon modes in wurtzite QW systems.

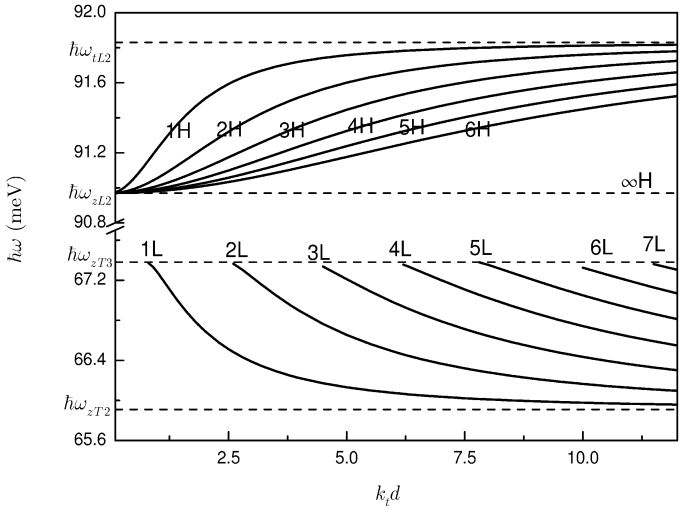

Fig. 2 The dispersion frequencies of the QC optical phonon modes $\hbar\omega$ as a function of the free wave-number in the xy plane k_t.

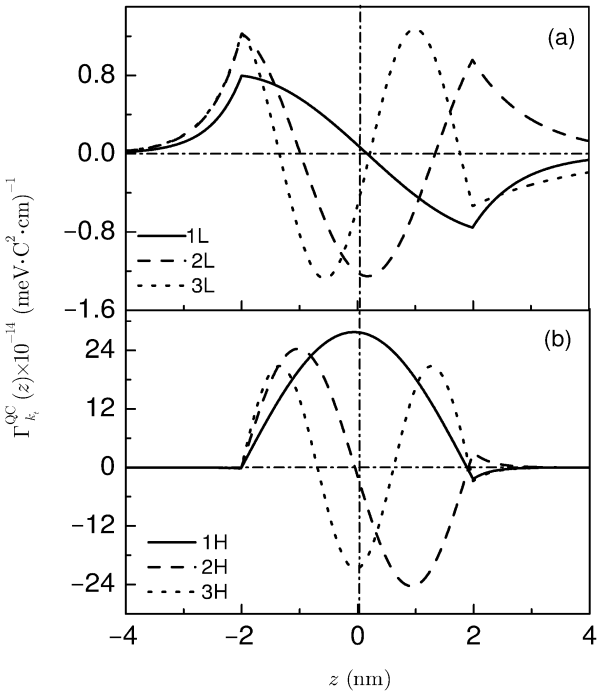

Fig. 3 The electron-QC phonon coupling functions $\Gamma^{\rm QC}_{\boldsymbol{k}_t}(z)$ as a function of z for the low frequency branches (a) and the high frequency branches (b) when $k_t d = 5$.

The electron-QC phonon coupling functions $\Gamma^{\rm QC}_{\boldsymbol{k}_t}(z)$ as a function of z are depicted for the lower frequency branches and the higher frequency branches when $k_t d = 5$ in Figs. 3(a) and 3(b), respectively. Via the figure, it is clear to see that, the distributions of the electrostatic potential for these QC phonon modes are neither symmetrical, nor antisymmetric, which is distinctly different from those in symmetric wurtzite QW systems.[6,24] Comparing Fig. 3(a) with Fig. 3(b), it is found that unsymmetries of the lower frequency branches of QC modes are more obvious than those of the high frequency branches of QC modes. On the other hand, the coupling strength of the higher frequency branches is nearly two-order magnitude high than that of the lower ones. We also observe that, the smaller the quantum number i is, the weaker the electron-phonon interaction of the low frequency branches becomes (Fig. 3(a)), but the stronger the electron-phonon interaction of the high frequency branches becomes (Fig. 3(b)). Furthermore, it is found that the damping of the electrostatic potential of the QC modes in the AlN barrier material is more quick than that in the $Al_{0.15}Ga_{0.85}N$ barrier material, which is due to the larger γ_1 than γ_3 for a same QC mode frequency ω (Refer to the ranges of $\omega_{z,T2}$–$\omega_{z,T3}$ and $\omega_{z,L2}$–$\omega_{t,L2}$ in Fig. 1). Via the discussion of electron-QC phonons coupling functions, it is found that the structural asymmetry also has significant influence on the electron-phonon interactions.[23]

Finally, we would like to mention the corresponding experiment works of QC and IO phonon modes in low-dimensional quantum systems, as well as the signification of theoretical results based on DC models for relative experimental data. Scamarcio *et al.*[29] experimentally observed the QC optical phonon modes in Si/GaAs SL systems by means of Raman spectroscopy. Syme, Lockwood and Baribeau[30] also confirm the existence of QC optic modes in a $(Si_{15}Ge_4)_{50}$ atom-layer SL. Dutta and coworkers[31] saw the IO modes in wurtzite GaN/AlN SLs via Raman scattering at room temperature, and they found that the frequency and the lineshape of phonon modes agree with predictions of the DC model. The group of Davydov[32] investigated the effects of the layer thickness and alloy composition on the Raman spectra of hexagonal nitride multilayer structures. Recently, Lazic

and collaborators[33] studied the influence of composition and strain in InGaN/GaN multi-layer QWs on the polar phonon frequencies using resonant Raman scattering technology. Gleize *et al.*[34,35] measured and recorded Raman spectra of IO modes and QC modes in GaN/AlN SL. Their experimental data of polar phonons angular dispersion in wurtzite heterostructures are found to be in good agreement with the results of a previous calculation based on DC model and Loudon's uniaxial crystal model. This illustrates that the DC model and Loudon's uniaxial crystal model are appropriate for the description of optical phonon modes in wurtzite heterostructures. However, to the best of our knowledge, the observation of QC optical modes in wurtzite asymmetric GaN/$Al_xGa_{1-x}N$ QW has not been reported in experiment by now. Thus at the moment, there are no available experimental data to contrast our theoretical results obtained in the present work. Of course, we hope that the present theoretical work could stimulate and guide further experimental investigations of the lattice dynamical properties in the asymmetric wurtzite heterostructures in the near future.

4 Summary

In conclusion, via the method of electrostatic potential expanding, the QC optical phonon modes and Fröhlich electron-QC optical phonon interactions in an asymmetric wurtzite QW are deduced and analyzed within the framework of the DC model and Loudon's uniaxial crystal model. Our theoretical scheme can be looked on as a generalization of the QC optical phonons in an ordinary wurtzite double heterostructures QWs, and it can be reduced to the situation of the symmetrical wurtzite QW once a set of symmetrical parameters are adopted.[6] The dispersion of the QC optical phonons and their electrostatic potential distributions for an asymmetric wurtzite QW is calculated numerically, and a detailed comparison with the situation of symmetric wurtzite QW is performed. Our results reveal that structural asymmetry of the wurtzite QW greatly influences the dispersion behaviors of the QC modes and the electron-QC phonon interaction coupling properties.

References

[1] B. Gil, *Group III Nitride Semiconductor Compounds*, Clarendon Press, Oxford (1998).

[2] S.M. Komirenko, K.W. Kim, M.A. Stroscio, and M. Dutta, Phys. Rev. B **59** (1999) 5013.

[3] J. Gleize, M.A. Renucci, J. Frandon, and F. Demangeot, Phys. Rev. B **60** (1999) 15985.

[4] B.C. Lee, K.W. Kim, M.A. Stroscio, and M. Dutta, Phys. Rev. B **58** (1998) 4860.

[5] J.J. Shi, Phys. Rev. B **68** (2003) 165335.

[6] L. Li, D. Liu, and J.J. Shi, Eur. Phys. J. B **44** (2005) 401.

[7] L. Zhang and H.J. Xie, J. Phys.: Condens. Matter **15** (2003) 5881.

[8] J. Licari, and R. Evrard, Phys. Rev. B **15** (1977) 2254.

[9] R. Fuchs, and K.L. Kliewer, Phys. Rev. **140** (1965) A2076.

[10] S.F. Ren, and Y.C. Chang, Phys. Rev. B **43** (1991) 11875.

[11] B. Zhu, Phys. Rev. B **44** (1991) 1926.

[12] L. Wendler, Phys. Status Solidi B **129** (1985) 513.

[13] N.C. Constantinou, and B.K. Ridley, Phys. Rev. B **41** (1990) 10622; 10627.

[14] R. Enderlein, Phys. Rev. B **47** (1993) 2162.

[15] K. Huang and B. Zhu, Phys. Rev. B **38** (1988) 13377.

[16] S.N. Klimin, E.P. Pokatilov, and V.M. Fomin, Phys. Status Solidi B **190** (1995) 441.

[17] H. Rücker, E. Molinari, and P. Lugli, Phys. Rev. B **44** (1991) 3463; **45** (1992) 6747.

[18] C.K. Sun, J.C. Liang, and X.Y. Yu, Phys. Rev. Lett. **84** (2000) 179.

[19] S. Tamura, D.C. Hurley, and J.P. Wolfe, Phys. Rev. B **38** (1988) 1427.

[20] C.E. Martinez, N.M. Stanton, P.M. Walker, *et al.*, Appl. Phys. Lett. **86** (2005) 221925.

[21] K.J. Yee, K.G. Lee, E. Oh, and D.S. Kim, Phys. Rev. Lett. **88** (2002) 105501.

[22] J.S. Im, H. Kollmer, J. Off, F. Scholz, and A. Hangleiter, Mater. Sci. Eng. B **59** (1999) 315.

[23] J.J. Shi, L. Shangguan, and S.H. Pan, Phys. Rev. B **47** (1993) 13471; J.J. Shi and S.H. Pan, Phys. Rev. B **51** (1995) 17681.

[24] P. Kinsler, R.W. Kelsall, and P. Harrison, Physica B **263-264** (1999) 507.

[25] V.N. Stavrou, M. Babiker, and C.R. Bennett. J. Phys.: Condens. Matter **13** (2001) 6489.

[26] A. Liu, S.L. Chuang, and C.Z. Ning, Appl. Phys. Lett. **76** (2000) 333.

[27] L. Zhang and H.J. Xie, Phys. Rev. B **68** (2003) 235315.

[28] J. Radovanovic, V. Milanovic, Z. Ikonic, and D. Indjin, Phys. Rev. B **69** (2004) 115311.

[29] G. Scamarcio, V. Spagnolo, E. Molinari, *et al.*, Phys. Rev. B **46** (1992) 7296.

[30] R.W.G. Syme, D.J. Lockwood, and J.M. Baribeau, Phys. Rev. B **59** (1999) 2207.

[31] M. Dutta, D. Alexson, L. Bergman, *et al.*, Physica E **11** (2001) 277.

[32] V. Yu. Davydov, A.A. Klochikhin, I.E. Kozin, *et al.*, Phys. Stat. Sol. A **188** (2001) 863.

[33] S. Lazic, M. Moreno, J.M. Calleja, *et al.*, Appl. Phys. Lett. **86** (2005) 061905.

[34] J. Gleize, F. Demangeot, J. Frandon, *et al.*, Phys. Status Solidi A **183** (2001) 157.

[35] J. Gleize, J. Frandon, Demangeot, M.A. Renucci, *et al.*, Mater. Sci. Eng. B **82** (2001) 27.